Enhanced performance of Al_2O_3-SiC-C castables via in-situ formation of multi-reinforced phasesby introducing surface treatedcomposite metal powders

QiulinXia[a], MeijieZhang[a*],HuazhiGu[a], Tingting Dong[a], Haifeng Li[b**], Mweemba Stephen[a], Chris R. Bowen[c]

[a]*The State Key Laboratory of Refractories and Metallurgy, Wuhan University of Science and Technology, Wuhan, China*

[b]*Engineering Research Center of Nano-Geomaterials of Ministry of Education, Faculty of Materials Science and Chemistry, China University of Geosciences, Wuhan, China*

[c]*Department of Mechanical Engineering, University of Bath, Bath BA2 7AY, UK; enskr@bath. ac. uk (K.R.)*

Corresponding Author:zhangmeijie@wust.edu.cn (M.J. Zhang);lihf@cug.edu.cn(H.F. Li)

Highlights:

1. 6.0-8.0 *wt.*% surface coated composite metal powders are introduced into ASC castables.
2. Multi-enhancement of whiskers/fibers are in suit formed due to coating cracked.
3. Comprehensive properties of ASC castables were greatly improved.

Abstract: Al_2O_3-SiC-C (ASC) castables were prepared with bauxite and silicon carbide as major raw materials and introducing large amount of surface treatedcomposite metal powders (STCMPs) as antioxidant. Their comprehensive properties were greatly improved attributed to the in situ formation of multi-reinforced phases including carbide silicon whiskers and mullite fibers in the matrix. Compared with the corresponding samples without STCMPs, the high temperature modulus of rupture of those with 6 *wt.*% STCMPs calcined in air increased by 47.3% and with 8 *wt.*% STCMPs calcined in reducing atmosphere increased by 220%. The retained CMOR ratio of the sample with 6 *wt.*% STCMPs calcined in reducing atmosphere was high up to 50% after 5 cycles thermal shocks. Moreover, the oxidation index and slag erosion index of samples with 6 *wt.*% STCMPs were decreased by 45% and 74%. This work provides a new perspective for the preparation of ASC castables with excellent high-temperature performance.

Keywords: Al_2O_3-SiC-C castables, Surface treated composite metal powders, Multi-reinforced phases, *In suit*formation

1. Introduction

Al_2O_3-SiC-C (ASC)castables are one of the primary refractory products used for molten iron pretreatment in iron and steel manufacturing process due to its excellent oxidation resistance and slagcorrosion resistance, thermal shockresistanceand good mechanical properties [1-3]. With the application and development of pretreatment desulfurization, dephosphorization and desiliconization technologies, higher requirements are demanded for ASC castables. Nevertheless,the high temperature oxidation of carbon (C) reduces the service life of ASC castables and limits their application[4-6]. As a result, to solve the issues, various methods and techniques have been developed, including changing the morphology of the introduced C such as graphitic carbon sphere[7],cobweb-like carbon nanotubes[8] and modified coal tar pitch[9],adding antioxidants such as andalusite [10, 11], Si_2BC_3N [12]and Al[13], and formation *in-situ* whiskers reinforcement[14-16].Among them, the most popular is adding metal and its alloy powders to ASC castables, which can not only improve its oxidation resistance, but also improve its toughness due to the reinforcing phases that were formed *in-situ* in ASC castables. For example, Sun *et al*. [17] found that the addition of 4 *wt.* % Al-Si powders improved the oxidation resistance of ASC bricks,and the generated whiskers improved the high temperature performance of the specimen. Behera *et al.*[18] found thatadding 2 *wt.*% Al powders as antioxidant in low-carbon magnesia-carbon bricksformed a ceramic phases*in situ* to improve the properties. Li *et al.*[19] found that the addition of 0.2 *wt.*% Al fibers improved the volume stability and mechanical strength of ASC castables. Li *et al.*[20] improved the thermal shock resistance of ASC castables by adding 2 *wt.*% of a composite antioxidant (Al, Si-based).In fact, when preparing ASC castables, the amount of untreated metal powders that can be added to ASC castables is very limited due to its easy hydration and significantly reduced flowability of ultra-low cement bonded ASC castables. Therefore, two issues must be considered to prepare ASC castables with excellent performance, namely, 1) hydration-resistance pretreatment of metal powders; 2) suitable addition amount of metal powders. As for the first aspect, in order to prevent its hydration, researchers have proposed solutions with preparing coatings on metal powders (*i.e.*, Al, Si powders).

In our previous studies [21], a Al_2O_3-coated Al powders were prepared and added to a Al_2O_3-SiO_2 refractory castable and its properties were greatly improved after heat-treatment at 1000 °Cin N_2 atmosphere. As for the second aspect, the addition of metal powders can not only improve the oxidation resistance of ASC castables, but also enhance its explosion resistance. Its anti-explosion mechanism is that the addition of metal powders increases the open pores or/and microcracks inside the ASC, which makes the steam in the ASC easily escape.However, previous studies have shown that adding metal powders can reduce the strength of castable although it has a good explosion resistance effect[22]. Therefore, in practical applications, the amount of metal powders added to ASC castables must be controlled to a very small level. For instance, Li *et al.*[19]investigated the effect of aluminum fiber addition (0.05, 0.1, 0.2, and 0.3 *wt.*%) on the mechanical strength and explosion resistance of ASC castables for iron runner. The results shown that the addition of metal aluminum fibers could effectively improve the explosion resistance and volume stability of ASC castables. The castables had better strength when metal aluminum fiber added was 0.10-0.20 *wt.*%. As is well-known, ASC castables are used in iron runner at temperatures above 1400°C, and its service conditions are very harsh.However, up to now, there are still few studies on the effect of adding a large doses of surface coated composite metal powders on the properties of ASC castables and the enhancement of their comprehensive high-temperature properties by *in-situ* formation of multi-reinforced phases.

In this study, sintered bauxite was used as raw material to prepare ASC castable for iron runner, and a large dose of surface treated composite metal powders (STCMPs) was added. The effects of STCMPs addition (0, 2, 4, 6 and 8 *wt.*%) and sintering atmosphere on the microstructure and its properties, including slag erosion resistance, oxidation resistance and thermal shock resistance were investigated. The results showed that the addition amount of STCMPs can be as high as 6.0-8.0 *wt.*%

and the physical properties, oxidation resistance, slag erosion resistance and thermal shock resistance of the castables were significantly improved.

2. Experimental Section

2.1 Raw materials

Bauxite particles ($w(Al_2O_3)$=85%, 0-1mm, 1-3mm, 3-5mm) and SiCparticles (w(SiC)=98%, 0-1mm, 1-3mm) were selected as aggregates. Bauxite powder ($w(Al_2O_3)$=85%, < 0.074mm), SiC powder (w(SiC)=98%, < 0.074mm), α-Al_2O_3 micro powder (D_{50} = 2.573 μm, Kaifeng Special Refractory Co., Ltd., Henan, China), spherical asphalt (w(C)=51.48%, Xinguang New Material Co., Ltd., Jiangsu China),and micro-silica (D_{50} =0.25μm) were chosen as the matrix materials. Calcium aluminate cement was used as the binder (D_{50}= 3.03 μm, Kerneos Aluminate Technologies, Tianjin, China). Composite metal powders including Al powder (D_{50} = 38 μm), Si powder (D_{50} = 38 μm) and metallic Al-12 *wt.*% Si powder (D_{50} = 38 μm) were used as the additives.

2.2. Preparation of ASC castables

Surface treated composite metal powders (STCMPs) were prepared by water vapor corrosion composed of 60 *wt.*% Al, 10 *wt.*% Si and 30 *wt.*% Al-Si alloy, which was referred to microcapsules in the following analysis. The process has been reported in detail in our previous work [21].The ratios of raw materials were determined according to the Andreasen packing model with a distribution coefficient of q=0.21, which is shown in Table 1.

Table 1 Compositions of prepared Al_2O_3-SiC-C castables

Samples / Raw materials	Contents, *wt.*%				
	S1	S2	S3	S4	S5
Bauxite particles	60	60	60	60	60
SiC particles	25	25	25	25	25
α-Al_2O_3micro powders	8	8	8	8	8
Spherical asphalt	3	3	3	3	3
Micro silica	1	1	1	1	1
Cement	3	3	3	3	3
STCMPs (extra)	0	2	4	6	8

The raw materials were mixed with water reducer (FS10, Wuhan Sanndar Chemical Company Co., Ltd, Wuhan,China) and about 5 wt.% water for all the samples, then they were cast into 140 × 25 × 25 mm^3 samples. The samples were cured at room temperature for 24 h, dried at 110 °C for 24 h and then calcined at 1450°C for 3h under an airor reducing atmosphere, respectively.

2.3. Characterization and measurement

The phases compositions of the samples were measured by X-ray diffraction (XRD, X'Pert Pro, PANalytical). The microstructures of calcined ASC castables were observed using a field-emission scanning electron microscope (FE-SEM, Nova Quanta 400) equipped with an energy-dispersive X-ray spectroscope (EDS, Phoenix, AMETEK Process Instruments).

The apparent porosity (AP), bulk density (BD), cold crushing strength (CCS) and cold modulus of rupture (CMOR) of the castables were measured according to GB/T 2997-2000 (China), GB/T 5072-2008 (China) and GB/T 3001-2007 (China), respectively.The high temperature modulus of rupture (HMOR) of calcined sampleswas measured under air atmosphere (GB/T 3002-2004, China). The samples were heated to 1400 °C at a rate of 5 °C/min and maintained for 0.5 h, then the HMOR was measured by the three-point bend test.The thermal shock resistance of the samples was evaluated using the water-cooling method (GB/T 30873-2014, China), between 1100 °C and 20 °C. After five thermal cycles, the residual $CMOR_{RS}$ of the samples was measured. The retained CMOR ratio (η) was calculated using the equation η= ($CMOR_{RS}$/CMOR) ×100%.Oxidation resistance of the sample was evaluated by the oxidation index (ω). The samples were heated to 1100°C for 5h under an air atmosphere [23], then naturally cooled to room temperature. The samples were then cut vertically from the middle section to observe the oxidation of carbon, according to the observed color change. The oxidized area (A_O) and the origin area (A_0) of samples were measured, then its oxidation index (ω) was calculated according to the equation, $\omega=A_O/A_0\times100\%$.The slag resistance was measured according tothe crucible method. The crucible sample (70mm×70mm×70mm), with a hole at the center, was filled with 20g of slag powders and fired at 1450°C for 3h. It was then cooled naturally and cut symmetrically to observe the degree of resistance to slag erosion. The erosion area (A_E) and the original area (A_S) of the crucible samples were measured, and its slag erosion index was then calculated according to the equation, $\delta=A_E/A_S\times100\%$. The chemical compositions of the blast furnace slag are shown in Table 2.

Table 2 Chemical compositions of blast furnace slag (*wt.*%).

Compositions	SiO_2	Al_2O_3	Fe_2O_3	CaO	MgO	K_2O	Na_2O	Others
Contents, *wt.*%	35.55	17.00	0.36	37.82	7.65	0.30	0.27	1.05

3. Results and discussion

3.1 Microstructure of calcined ASC castables

The XRD patterns of samplescalcined in the air/reducing atmosphere are shown in Fig. 1. The results in Fig.1 shown that the major phases of the calcined samples in both air and reducing atmosphere were corundum (Al_2O_3, ICDD No. 00-048-0366, ICDD No. 01-082-1399, ICDD No. 01-075-0783, ICDD No. 00-005-0712) and alphasilicon carbide (α-SiC, ICDD No. 01-073-2086, ICDD No. 01-073-1663, ICDD No. 01-073-1663, ICDD No. 01-089-1975), and contain a small amount of mullite ($3Al_2O_3·2SiO_2$, ICDD No. 01-082-1237), carbon and calcium-aluminum-silicon complex oxides. Fig.2 shows FESEM images and EDS analysis of calcined products of ASC castables with different amounts microcapsules added in air atmosphere of 1450°C. As can be seen, only a small number of needle-like and rod fibers were observed in calcined ASC castables without microcapsules added.Microcracks were found in the calcined ASC castables with microcapsule addition, and even breakages.Meanwhile, with the addition of SCCMP microcapsules in the samples, whiskers/fibers network structure appeared around the microcapsule cracks, as shown in Fig. 2 (b). As the number of microcapsules in the sample increased from 2 *wt.*% to 8 *wt.*% (Fig. 2 (b-e)), the number of whiskers/fibers increased around the microcapsules which expanded into the matrix and formed a network. The pores in the matrix were filled with whiskers/fibers and connect to each other to form an interconnected network. Compared with that of the samples without microcapsules added, the samples with the microcapsules added had whiskers/fibers with smaller diameters and longer length,as shown in Fig. 2 (b)-(e).

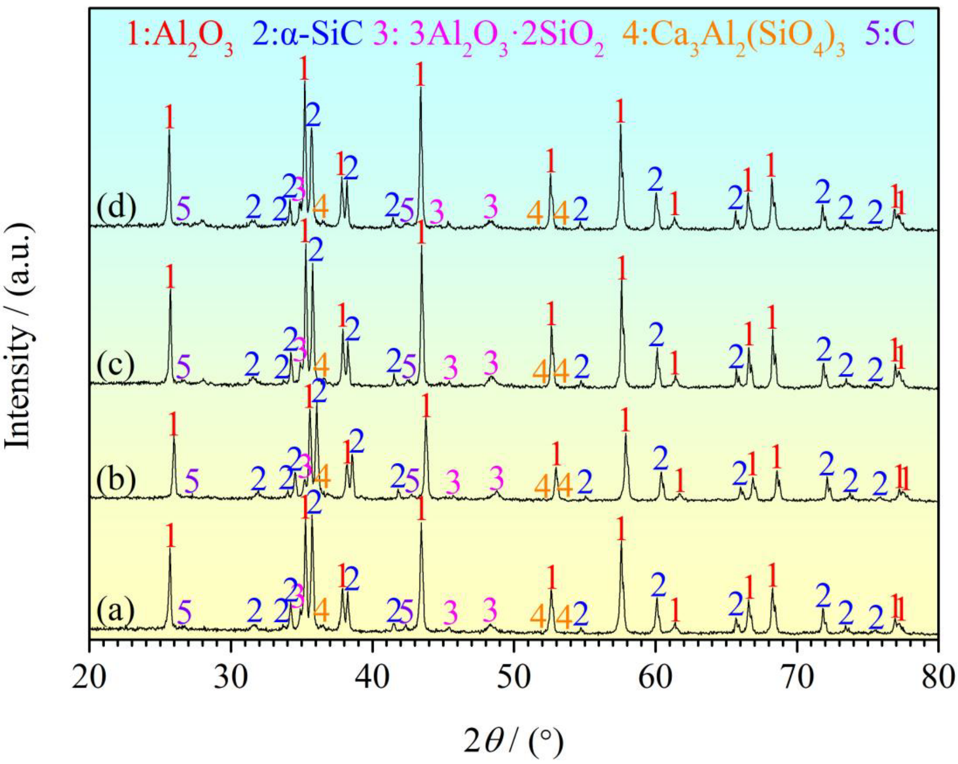

Fig. 1. XRD patterns of calcined products of ASC castables at 1450°C with (a and c) 0 *wt.*%,

(b and d) 6 *wt.*% microcapsules added in (a and b) air atmosphere and (c and d) reducing atmosphere, respectively.

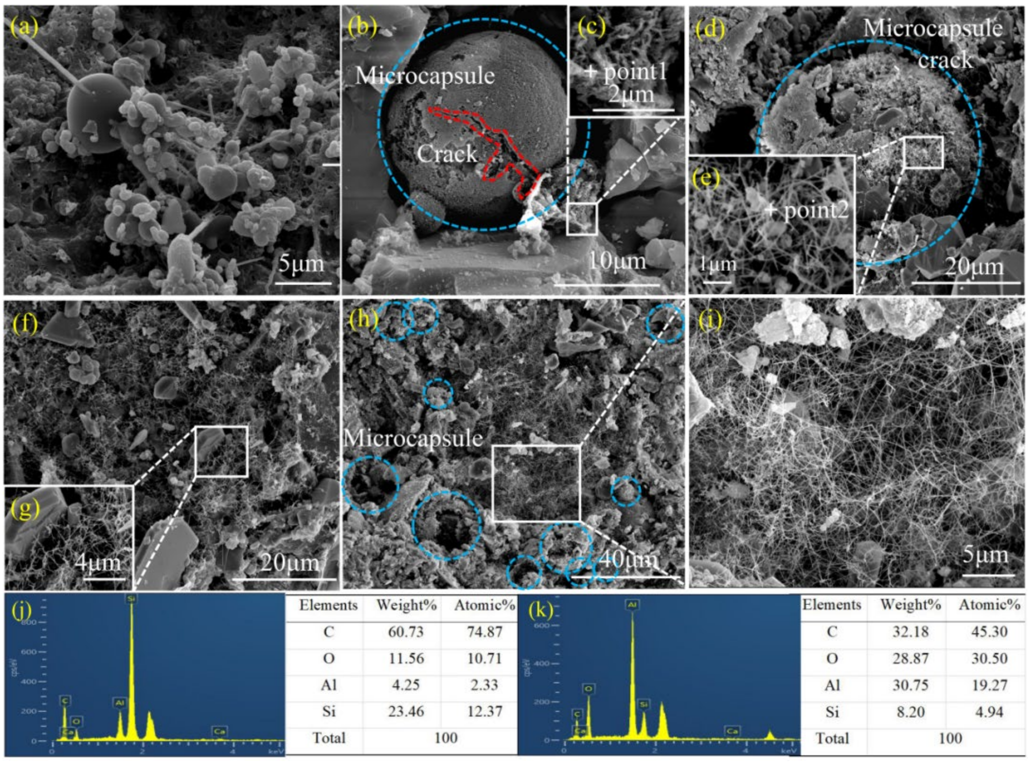

Fig. 2. FESEM images of calcined products of ASC castables at 1450°C in air atmosphere with (a) 0 *wt.*%, (b and c) 2 *wt.*%, (d and e) 4 *wt.*%, (f and g) 6 *wt.*% and (h and i) 8 *wt.*% microcapsules added. EDS of (j) point 1# and (k) point 2# of ASC castables calcinated at 1450°C in air atmosphere.

Compared with the samples fired in an air atmosphere (Fig. 2(a)), no whiskers/fibers appear in without any microcapsules added samples calcined at 1450°C in reducing atmosphere, as shown in Fig. 3(a). A small number of short rod-shaped fibers appear in the sample with 2 *wt.*% microcapsules, as shown in Fig. 3(b). Some whisker/fibers appear within the cracked microcapsule zone when the content of the microcapsules is increased to 4 *wt.*% (Fig. 3(c)). When the content of the microcapsules is further increased to 6*wt.*%, more whiskers/fibers appear in the matrix and some grow longer (Fig. 3 (d), (e)). By comparison, it was found that the microstructure of ASC castables was obviously different when the same number of microcapsules were added and calcined in reducing atmosphere and air atmosphere respectively. The most apparent difference was that the fiber/whisker generated in reducing atmosphere was less and the aspect ratio was much smaller. Clearly, it can be seen that the number of fibers/whiskers formation and the aspect ratio are sensitive to the calcination atmosphere. During calcination in reducing atmosphere, the amount of SiO (g) and CO (g) is insufficient due to the low oxygen pressure, resulting in a small number of fibers/whiskers, which is consistent with the results of previous studies [24, 25].

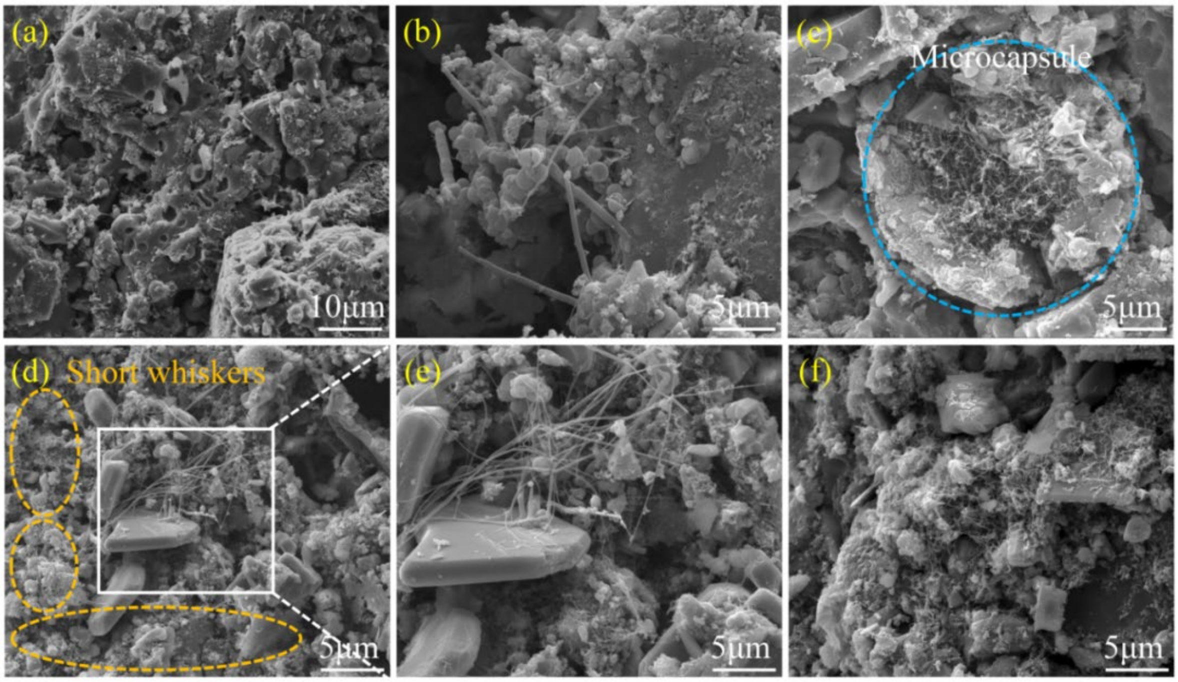

Fig. 3. FESEM images of calcined products of samples at 1450°C in reducing atmosphere with (a) 0 *wt*.%, (b) 2 *wt*.%, (c) 4 *wt*.%, (d and e) 6 *wt*.% and (f) 8 *wt*.% microcapsules added.

FactSage software was used to calculate the Predominance diagram of the Al-Si-O-C system at 1450°C to evaluate the effects of partial pressure of CO (P_{CO}) and O_2(PO_2) on the chemical reactions and product phases of the system, as shown in Fig. 4.It can clearly be seen that when both P_{CO} and P_{O_2} partial pressures were low (phase region ①), Al and Si existed simultaneously and no new phase was formed.Meanwhile, SiC and Al_4C_3 phases appeared with the increase of P_{CO}, while Al_2O_3 phase appeared with the increase of P_{O_2}. That is, the Al_2O_3 or/and SiC new phases could be formed in Al-Si-C-O reaction system in oxidizing or reducing atmosphere when partial pressures P_{CO} and P_{O_2} were appropriate. As shown in Fig.1, Al and Si were absent in the system in either oxidizing or reducing atmosphere. Besides, considering the EDS analysis of point 1# and point 2# (Fig. 2), the predominance diagram of Al-Si-O-C system at 1450˚C (Fig. 4), and the crystallization behavior of silicon carbide(SiC) and mullite($3Al_2O_3{\cdot}2SiO_2$, A_3S_2), it can thus be concluded that SiC whiskers (SiC_w) and mullite fibers ($A_3S_{2,f}$) was generated in ASC castables.And, the schematic of the formation mechanism of whiskers/fibers is shown in Fig. 5.The formation of SiC_w and $A_3S_{2,f}$ can be considered as: (i) Microcapsules in ASC castables cracked at high temperature, and exposed Si and Al react with O_2 in the surrounding atmosphere to form SiO (g) and Al_2O_3 (s), respectively. (ii) Then, the reaction intermediates SiO (g) reacted with C (s) or CO (g) to form SiC_w, while SiO (g) reacted with Al_2O_3 (s) to form $A_3S_{2,f}$. Therefore, it can be predicted that SiC_w and $A_3S_{2,f}$ *in-situ* formation can improve the comprehensive properties of ASC castables.

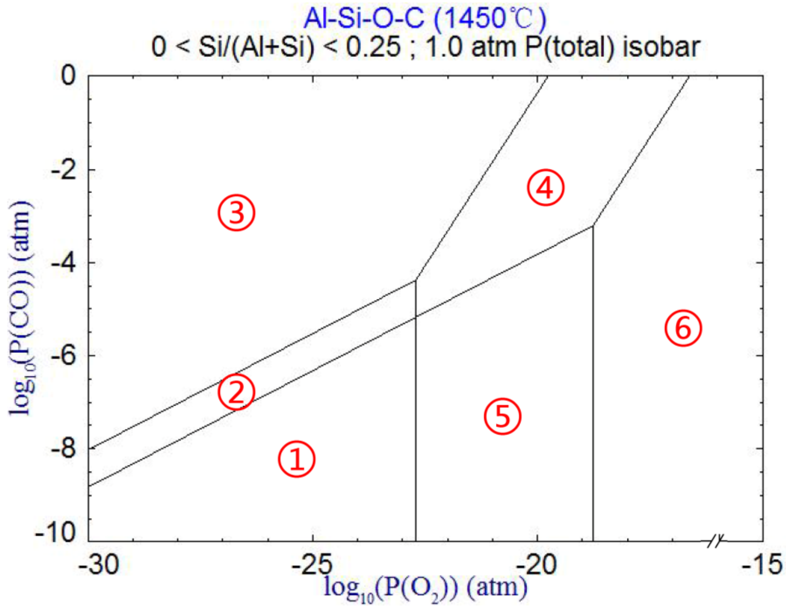

Fig. 4. Predominance diagram of Al-Si-O-C system at 1450°C calculate by FactSage software. ① Al(l)+Si(l), ② Al(l)+SiC(s), ③ Al_4C_3(s)+SiC(s), ④Al_2O_3(s)+SiC(s),⑤Al_2O_3(s)+Si(l), ⑥ Al_2O_3(s)+$3Al_2O_3 \cdot 2SiO_2$(s).

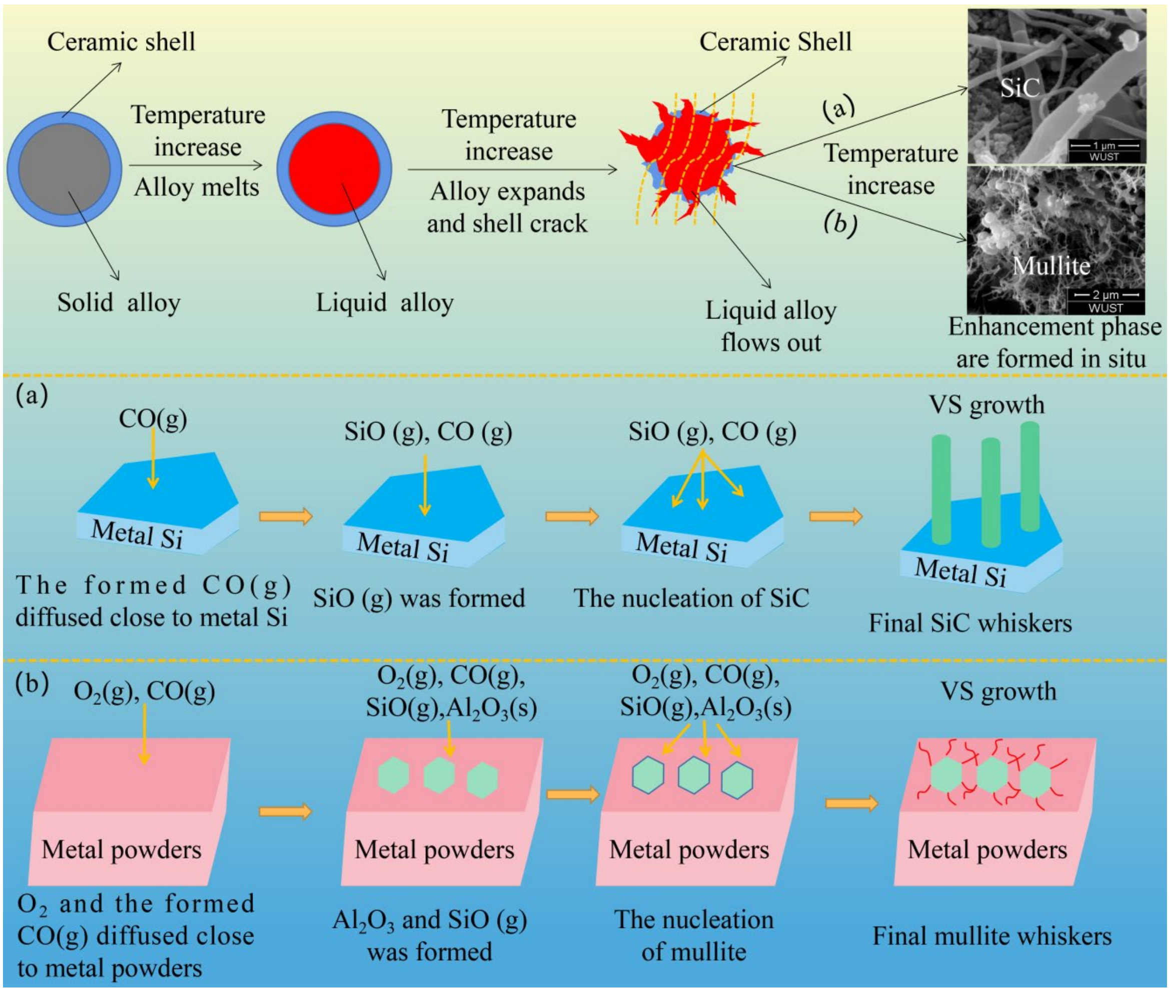

Fig. 5. Schematic illustration of formation mechanism of (a) silicon carbide whiskers and (b)

mullite whiskers during high temperature calcination.

3.2. Effects of microcapsules amount on properties of ASC castables

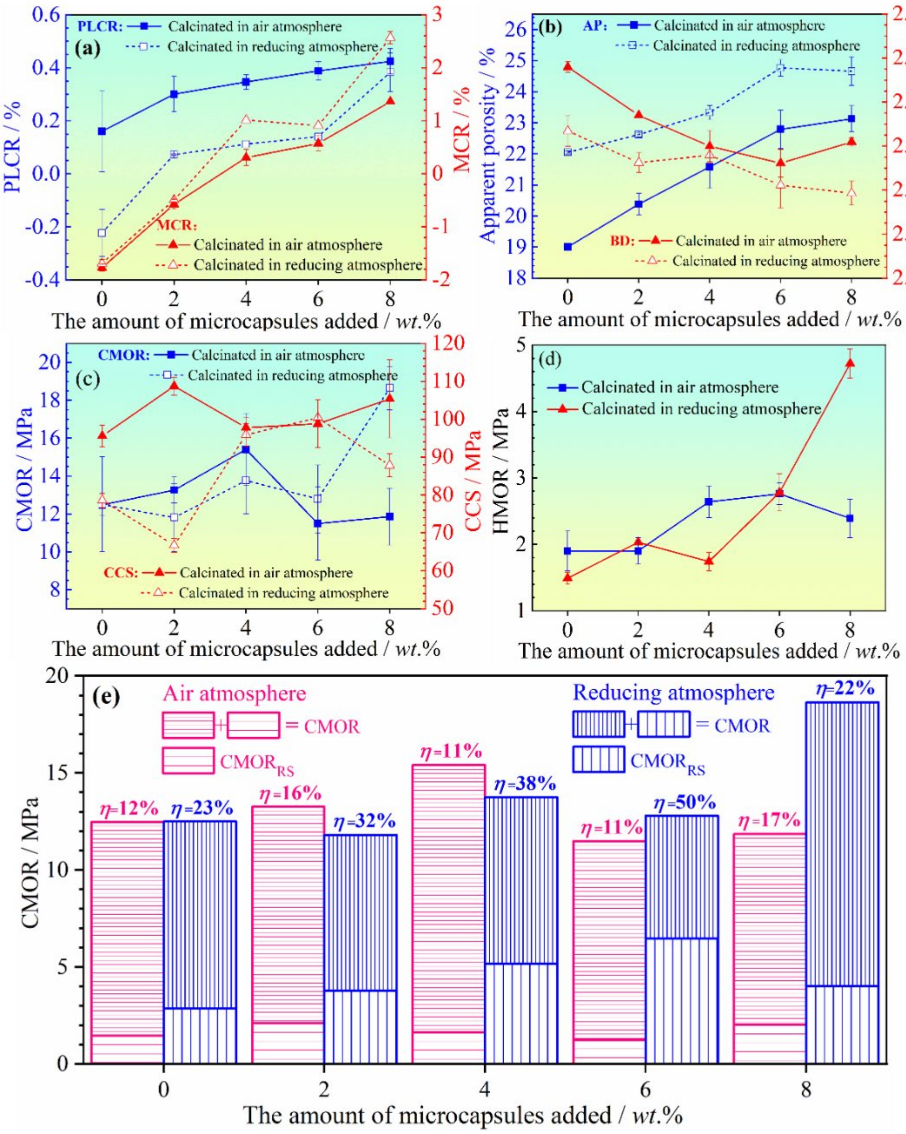

Fig. 6.Effect of microcapsules amount on properties (a) PLCR and MCR, (b) AP and BD, (c) CMOR and CCS, (d) HMOR of samples calcined in air/reducing atmosphere. (e) Effect of microcapsules amount and sintering atmosphere on the CMOR, $CMOR_{RS}$ and η of samples after thermal shock resistance 5 cycles.

The mass change ratios (MCR) and permanent linear change ratios (PLCR) of samples calcined in air or reducing atmosphere are shown in Fig. 6 (a). It can be seen that the addition of microcapsules can compensate for the weight loss of ASC castables during high-temperature calcination. For the ASC castables sintered samples without microencapsulation added, there was a slight weight loss of -1.80 *wt*.% due to the high temperature oxidation of SiC and spherical asphalt. However, for the samples with microencapsulation added, the weight loss was compensated to some extent by the high temperature oxidation of exposed Al and Si due to microcapsule rupture. When the microcapsule addition amount was 4 *wt*.%, the weight gain of metal oxidation was slightly greater than the weight loss of the system, and when the microcapsule content was 8 *wt*.%, the weight gain of sintering products in oxidizing and reducing atmosphere was about 1.4% and 2.6%, respectively. The weight gain of the latter was greater than that of the former due to the less weight loss in reducing atmosphere. Meanwhile, the PLCR of the calcined samples without microencapsulation added calcined in oxidizing andreducing atmosphere was about –0.23% and 0.18%, respectively. This is mainly because SiC is oxidized to form SiO(g) and SiO_2(g) under oxidizing atmosphereaccompanied by volume expansion, while the sample mainly produces shrinkage by sintering densification under reducing atmosphere. The PLCR of the calcined samples with microencapsulation added shows an increasing trend but all are less than 5%. This is mainly due to the high temperature expansion of microcapsules.The small volume expansion due to oxidation helped to maintain the structural stability of ASC castables.The apparent porosity (AP) and bulk density (BD) of samples calcined in air or reducing atmosphere are shown in Fig.6(b).With the increase of microcapsules content, AP of ASC castables increased, while BD decreased. The increase of AP was caused by the rupture of microcapsules, Al and Si oxidation and the *in-situ* formation of whiskers and fibers, while the decrease of BD was due to the expansion of its volume more significant than its weight change. The cold modulus of rupture (CMOR),cold crushing strength (CCS) and high temperature modulus of rupture (HMOR) of samples calcined at 1450 °Cin air and reducing atmosphere are shown in Fig. 6 (c) and Fig. 6 (d), respectively.As can be seen from Fig. 6 (c), when the addition number of microcapsules was greater than 4 *wt*.%, the CCS of the samples calcined in oxidizing atmosphere and reducing atmosphere basically remained at ~100 MPa. However, when the addition amount is 8 *wt*.%, the CCS of the samples calcined in oxidizing atmosphere slightly increased while that of the samples calcined in reducing atmosphere slightly decreased. This may be caused by the poor sintering effect of the latter, which was also consistent with the results in Fig. 6 (b). Simultaneously, the CMOR of all samples basically remained at about 13 MPa. When the addition number of microcapsules varied between 4 – 8 *wt*.%, the CMOR of samples calcined in oxidizing atmosphere or reducing atmosphere showed a trend of first decreasing and then increasing. In addition, as shown in Fig. 6 (d), the HMOR of all samples calcined in oxidizing atmosphere or reducing atmosphere increased with the increase of microcapsule addition amount, except that HMOR of samples with 8 *wt*.% microcapsule addition amounts in oxidation atmosphere decreased slightly. Besides, the HMOR of the sample with 6 *wt*.% microcapsules addition calcined in oxidizing atmosphere was 2.8 MPa, which was 47.3% higher than the corresponding HMOR value of 1.9 MPa of the blank sample. Moreover, the HMOR of the sample with 8 *wt*.% microcapsule addition calcined in reduction atmosphere was 4.8 MPa, which was 220% higher than the corresponding HMOR value of the blank sample of 1.5 MPa.Fig. 6 (e) shows the effect of microcapsules amount and sintering atmosphere on the CMOR, $CMOR_{RS}$ and η of samples after thermal shock resistance 5 cycles. For ASC castables calcined in oxidizing or reducing atmosphere with different microcapsules added, the CMOR range of the samples subjected to 5 cycles thermal shocks was 1.25 – 2.10 MPa and 2.87 – 6.45 MPa, respectively. The η value of the samples calcined in the oxidizing atmosphere after 5 cycles thermal shocks had a small variation range, all within 11–17%. However, the η value of the samples calcined in reducing atmosphere after 5 cycles thermal shocks varied from 20% to 50%. In particular, the η value of the sample calcined in reducing atmosphere with 6 *wt*.% microcapsule addition was up to 50% after 5 cycles thermal shocks, showing excellent high temperature performance. Therefore, it is concluded that the addition of microcapsules improved the comprehensive properties of ASC castables.

3.3. Oxidation resistance and slag resistance of ASC castables

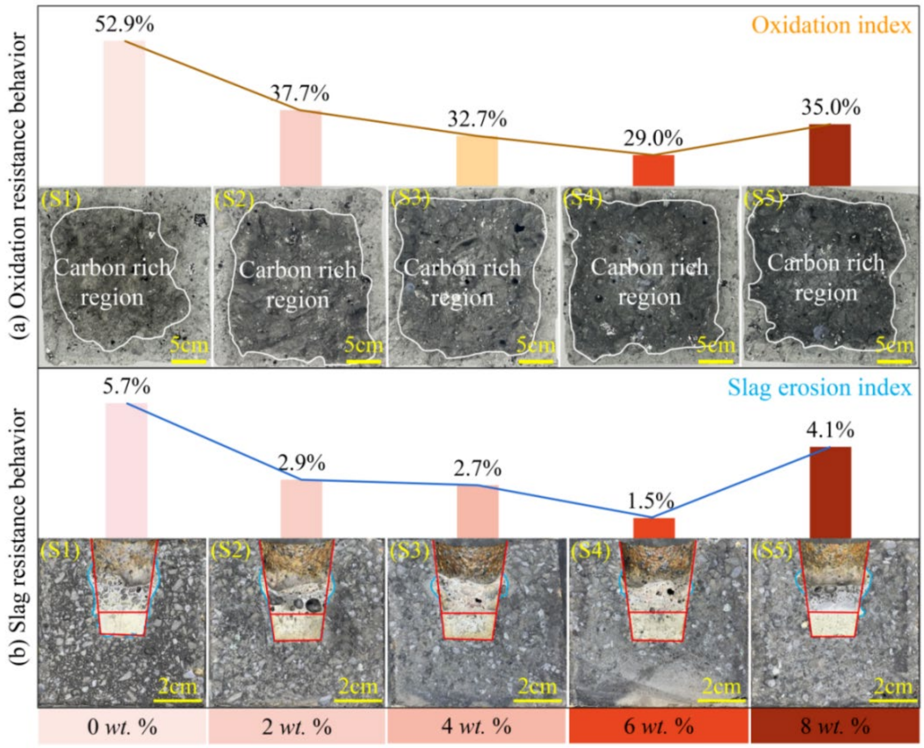

Fig. 7. Effects of the addition of microcapsule on oxidation resistance and slag resistance of ASC castables. (a) Oxidation resistance behavior contains cross-sectional images and oxidation index of samples calcined at 1100°C for 3 h in an air atmosphere and (b) Slag resistance behavior contains digital photographs of cross sections of crucibles and slag erosion index after slag corrosion at 1450°C for 3 h.

Oxidation resistance behavior contains cross-sectional images and oxidation indexof samples calcined at 1100°C for 3h in an air atmosphereare shown in Fig. 7 (a). To observe the oxidation of the samples more clearly, the samples were divided into a non-oxidised region (carbon-rich area) and an oxidised region (gray area). With the increase of microcapsules addition, the non-oxidised region area of the samples initially increased and then decreased.Even if the number of microcapsules was 8 *wt.*%, the non-oxidized zone area of the sample was still much larger than that of the materials without microcapsules. In addition,the oxidation index of the sample without microcapsules is the largest, while the oxidation index of the sample with 6 *wt.*% microcapsules is the smallest which decreased by 45% compared with the former.This is supposed to be because the microcapsules break up at high temperature and the exposed Al and Si reacts preferentially with oxygen, protecting the carbon. However, when the addition of microcapsulesexceeded 8 *wt.*%, itsAPand internal defectsbecame larger, which was not conductive to improving the oxidation resistance of samples.

Table 3 Comparison of properties of ASC castables with different antioxidant types and addition amount.

Antioxidant	Species	$(Si+BC_4)$ $+Si_2BC_3N$	Si	Si + Graphitic carbon spheres	$Al+Si+Al_2O_3$–B_2O_3 composite	STCMPs
	Addition amounts	2.8 *wt.*% +0.5 *wt.*%	1.5 *wt.*%	2.0 *wt.*% +2.0 *wt.*%	0.01 *wt.*% + 0.01 *wt.*% + 2.0 *wt.*%	**4 - 8 *wt.*%**
Samples preparation conditions		1400 °C ×3 h	1500 °C× 3 h	1450 °C × 3 h	1500 °C× 3 h	1450 °C× 3 h
CMOR, MPa	Air atmosphere	13 MPa	14.5 MPa	7.4 MPa	9.93 MPa	**15.40** MPa
	Reducing atmosphere	16.3 MPa	17.7 MPa	-	-	**19.0**MPa
Thermal shock resistance	Conditions	1 cycle, 900 °C×30 min	1 cycle, 1100 °C×30 min	3 cycles, 1100 °C×20 min	-	**5** cycles, 1100 °C × 30 min
	Air atmosphere	65.9%	28.2%	28.5 %	-	17%
	Reducing atmosphere	-	34.3%	-	-	**50%**
HMOR, MPa	Conditions	1400 °C×0.5 h	1400 °C× 1.0 h	1450 °C× 0.5 h	1450 °C× 0.5 h	1400 °C× 0.5 h
	Air atmosphere	3.15 MPa	3.25 MPa	4.7 MPa	1.67 MPa	2.8 MPa
	Reducing atmosphere	2.6 MPa	3.5 MPa	-	-	**4.8**MPa
Oxidation index		-	-	-	28.9 %	29%, 1100°C×5 h
Slag erosion index		-	-	-	-	**1.5%**, 1450°C× 3h

Main raw materials	Brown alumina, SiC	Brown fused alumina, SiC	Brown fused alumina, SiC	Brown alumina, SiC	**Bauxite**, SiC
Refs.	[10]	[21]	[6]	[5]	***this work***

Slag resistance behavior contains digital photographs of cross sections of crucibles and slag erosion indexafter slag corrosion at 1450°C for 3hare shown in Fig. 7(b). The five crucible samples remained intact after the slag resistance test and the interface between the slag and the crucible was clearly distinguished. Severe corrosion occurred mainly at the three-phases junction of air-slag-sample, especially for the sample without microcapsules added.It can be seen from Fig. 7(b) that the sample without the microcapsules had the largest slag erosion index while the sample with 6*wt*.% microcapsulesshowed the best slag erosion resistance. Since this sample had the best oxidation resistance, there was more graphite as well as whiskers/fibers in their matrix, which improved its slag erosion resistance.

The performance comparison of ASC castables with different raw materials, antioxidant types and addition amount, as summarized in Table 3.Under the condition that the main raw material was bauxite and the dosage was up to 60 *wt*.%, the ASC castables prepared in this study had outstanding comprehensive properties. The results showed that adding surface coated microcapsules was a feasible way to improve the performance of ASC castables.

4. Conclusion

Surface treated composite metal powders (microcapsules) were prepared and added to Al_2O_3-SiC-C refractory castables, and the following conclusions were obtained:

(1) SiC and mullite whiskers/fibers are formed *in-situ* at high temperature when the microcapsules are added to Al_2O_3-SiC-C castables, which greatly promotes the cold modulus of rupture (CMOR), cold crushing strength (CCS) and high temperature modulus of rupture (HMOR).

(2) Compared with the corresponding samples without surface treated composite metal powders, the high temperature modulus of rupture (HMOR) of the calcined samples with 6 *wt*.% STCMPs addition in oxidizing atmosphere and 8 *wt*.% STCMPs addition in reducing atmosphere increased by 47.3% and 220%, respectively.

(3) The oxidation index and slag erosion index decrease by 45% and 74% respectively for the samples with 6 *wt*.% STCMPs, compared with the microcapsule free material.

CRediT authorship contribution statement

Qiulin Xia: Investigation, Writing-original draft.**Meijie Zhang**: Supervision, Methodology, Conceptualization, Project administration, Funding acquisition, Writing-review & editing.**Huazhi Gu**: Methodology, Supervision. **Wuguo Xiang**: Investigation. **Tingting Dong**: Investigation. **Haifeng Li**: Writing-review & editing, Formal analysis, Methodology.**Mweemba Stephen**: Writing-review & editing. **Chris R. Bowen**:Writing-review & editing.

Declaration of competing interest

The authors declare that they have no known competing financial interests or personal relationships that could have appeared to influence the work reported in this paper.

Acknowledgements

The authors appreciate the financial support from the National Natural Science Foundation of China (Grant No. 52072276) and theFoundation of Huzhou Municipal Science and Technology Bureau,Zhejiang Province (Grant No. 2020ZD2016).

References

[1] Yang S, Xiao G, Ding D, et al. Improved corrosion resistance of Al_2O_3-SiC-C castables through in situ carbon containing aluminate cement as binder. International Journal of Applied Ceramic Technology, 2020, 17(3): 1044-1051. https://doi.org/10.1111/ijac.13474

[2] Wu J, Bu N, Li H, et al. Effect of B_4C on the properties and microstructure of Al_2O_3-SiC-C based trough castable refractories. Ceramics International, 2017, 43(1): 1402-1409. https://doi.org/10.1016/j.ceramint.2016.10.101

[3] Shan J, Li Y, Liao N, et al. Critical roles of synthetic zeolite on the properties of ultra-low cement-bonded Al_2O_3-SiC-C castables. Journal of the European Ceramic Society, 2020, 40(15): 6132-6140. https://doi.org/10.1016/j.jeurceramsoc.2020.07.035

[4] Chen A, Fu Y, Mu Y, et al. Oxidation resistance of andalusite-bearing Al_2O_3-SiC-C castables containing reduced anti-oxidant. Ceramics International, 2021, 47(10): 14579-14586. https://doi.org/10.1016/j.ceramint.2021.02.039

[5] Li M, Tong S, Luo H, et al. Dual-functional application of Al_2O_3-B_2O_3 composite bubble in Al_2O_3-SiC-C castables as antioxidant and mechanical reinforcement agents[J]. Ceramics International, 2021.https://doi.org/10.1016/j.ceramint.2021.05.077

[6] Yin Y, Wang S, Zhang S, et al. Preparation of SiC coated graphite flake with much improved performance via a molten salt shielded method[J]. International Journal of Applied Ceramic

Technology, 2022, 19(3): 1529-1539. https://doi.org/10.1111/ijac.13961

[7] Li S, Liu J, Wang J, et al. Catalytic preparation of graphitic carbon spheres for Al_2O_3-SiC-C castables. Ceramics International, 2018, 44(11): 12940-12947. https://doi.org/10.1016/j.ceramint.2018.04.108

[8] Zang Y, Xiao G, Ding D, et al. Study on cobweb-like carbon nanotubes/calcium aluminate cement and its effect on the properties of Al_2O_3-SiC-C castables. International Journal of Applied Ceramic Technology, 2022, 19(1): 557-568.https://doi.org/10.1111/ijac.13905

[9] Wang S, Zhou P, Liu X, et al. Effect of modified coal tar pitch addition on the microstructure and properties of Al_2O_3-SiC-C castables for solid waste incinerators[J]. Ceramics International, 2022. https://doi.org/10.1016/j.ceramint.2022.04.060

[10] Chen A, Wang X, Zhou W, et al. Oxidation resistance of Al_2O_3-SiC-C castables with different grades of andalusite. Journal of Alloys and Compounds, 2021, 851: 156836. https://doi.org/10.1016/j.jallcom.2020.156836.

[11] Tian X, Liu M, Luan J, et al. Effects of andalusite aggregate pre-fired at different temperatures on volume stability and oxidation resistance of Al_2O_3-SiC-C castables. Ceramics International, 2020, 46(14): 22745-22751. https://doi.org/10.1016/j.ceramint.2020.06.041

[12] Shan J, Liao N, Li Y, et al. Influences of novel Si_2BC_3N antioxidant on the structure and properties of Al_2O_3-SiC-C castables: In air and coke bedded atmosphere. Ceramics International, 2019, 45(3): 3531-3540. https://doi.org/10.1016/j.ceramint.2018.11.011

[13] Venkata Siva S B, Ganguly R I, Srinivasa Rao G, et al. Quantitative studies on wear behavior of Al-(Al_2O_3-SiC-C) composite prepared with in situ ceramic composite developed from colliery waste. Proceedings of the Institution of Mechanical Engineers, Part J: Journal of Engineering Tribology, 2015, 229(7): 823-834.https://doi.org/10.1177/1350650115570696.

[14] Lian J, Zhu B, Li X, et al. Effect of in situ synthesized SiC whiskers and mullite phases on the thermo-mechanical properties of Al_2O_3-SiC-C refractories. Ceramics International, 2016, 42(14): 16266-16273. https://doi.org/10.1016/j.ceramint.2016.07.163.

[15] Xing H, Zou B, Wang X, et al. Fabrication and characterization of SiC whiskers toughened Al_2O_3 paste for stereolithography 3D printing applications. Journal of Alloys and Compounds, 2020, 828: 154347.https://doi.org/10.1016/j.jallcom.2020.154347.

[16] Liu X, Huang Y, Sun J, et al. Formation and growth of in-situ SiC nanowires in Al_2O_3-C materials under various atmospheres[J]. Ceramics International, 2020, 46(17): 27750-27757.

https://doi.org/10.1016/j.ceramint.2020.07.274
[17] Sun Xiaoting, Tian Lin, Chen Shujiang, et al. Effect of Composite Antioxidant on properties of Al_2O_3-SiC-C brick. Bulletin of the Chinese Ceramic Society, 2017, 36(11): 3932-3935, 3943.
[18] Behera S, Sarkar R. Effect of different metal powder anti-oxidants on N220 nano carbon containing low carbon MgO-C refractory: An in-depth investigation. Ceramics International, 2016, 42(16): 18484-18494. https://doi.org/10.1016/j.ceramint.2016.08.185
[19] Li Y, Zhao H, Zhang H, et al. Enhancement and explosion-proof mechanism of aluminum fiber addition in Al_2O_3-SiC-C castables for iron runner. Ceramics International, 2019, 45(17): 22723-22730. https://doi.org/10.1016/j.ceramint.2019.07.310
[20] Li Yaxiong, Li Xiangcheng, Zhu Boquan. Effect of composite antioxidant additions on properties of Al_2O_3-SiC-C castables. Naihuo Cailiao, 2013, 47(5): 345-347.
[21] Xia Q, Zhang X, Zhang M, et al. Improvements of properties of alumina-silica refractory castables by alumina-coated aluminum powders [J]. Journal of Alloys and Compounds, 2020, 832: 154925. https://doi.org/10.1016/j.jallcom.2020.154925
[22] Cheng S, Zhao H, Wang Y, et al. Submicron SiO_2 Powder: Characterization and Effects on Properties of Cement-Free Iron Ditch Castables. Advances in Materials Science and Engineering, 2021, 2021.
[23] Zhao Chunyan, Chen Maofeng, QianZhongjun, et al. Effects of carbon source on properties of Al_2O_3-SiC-C iron trough castables [J]. NAIHUO CAILIAO, 2021,55(1):56-60.
[24] Zhou P, Qiu X, Luo Z, et al. Effect of firing atmosphere on the microstructure and properties of Al_2O_3-SiC-C castables [J]. Ceramics International, 2021, 47(10): 14280-14289. https://doi.org/10.1016/j.ceramint.2021.01.290
[25] Wei J, Li K Z, Li H J, et al. Growth and morphology of one-dimensional SiC nanostructures without catalyst assistant [J]. Materials chemistry and Physics, 2006, 95(1): 140-144. https://doi.org/10.1016/j.matchemphys.2005.05.032